Colloid and Interface Science Communications 52 (2023) 100686

Contents lists available at ScienceDirect

Colloid and Interface Science Communications

journal homepage: www.elsevier.com/locate/colcom

Dispersibility study of carbon nanotubes using multiple light scattering: A mini-review

Hyungsub Yoon [a], Russ Thompson [b], Byungil Hwang [a,*]

[a] School of Integrative Engineering, Chung-Ang University, Seoul 06974, Republic of Korea
[b] Crystallize 4Cs Limited, UK

ARTICLE INFO

Keywords:
Dispersibility
Carbon nanotube
Battery
Multiple light scattering

ABSTRACT

Carbon nanotubes (CNTs) are used as conduction materials for cathodes or anodes of secondary batteries. The dispersibility of CNTs in a solvent is a crucial property for producing high-efficiency CNT-based batteries because the battery performance depends on the CNT density in the electrodes. Measuring small changes in the dispersion state of CNTs in solution, depending on the dispersion method, is essential to obtain highly stable CNT dispersions. The multiple light scattering can effectively characterize the CNT dispersibility, taking advantage of its ultrahigh-resolution light detection and time-dependent measurement abilities. Although some studies of CNT dispersibility using the multiple light scattering have been reported, a comprehensive review of these results is still lacking. This mini-review introduces the fundamental principles of the multiple light scattering. We summarize research trends on measuring CNT dispersibility using this method, focusing on the strategies used for preparing stable CNT dispersions.

1. Introduction

The various advantages of carbon nanotubes (CNTs), such as excellent mechanical properties, high electrical conductivity, and outstanding thermal properties, have attracted considerable attention in several application areas, such as novel sensors [1–6], memory or computing devices [7–13], fifth-generation (5G) antennae [14–19], and secondary batteries [20–29]. Their application as conductive additives for anode or cathode materials is of particular interest to engineers or researchers in the lithium-ion battery industry, owing to the potential for enhancing the energy density of batteries [30–34]. In addition, the excellent mechanical properties of CNTs reduce fractures in silicon anodes during charge/discharge cycles, enhancing the stability of batteries based on these anodes [27,31,35,36].

The performance of batteries using CNTs is primarily governed by the densities of the CNTs in the total electrode volume [37–40]. A higher amount of CNTs in the electrodes leads to an improved battery efficiency. However, as the volume of the electrode is limited, the content of CNTs cannot be increased indefinitely. In addition, the CNTs have an intrinsic tendency to agglomerate in water or organic solvents, which reduces their performance and amount available for incorporation into electrode mass [41–45]. Effective dispersion methods enhance the formation of concentrated CNT dispersions. There is a direct relationship between concentration of CNT in a dispersion and density of CNT in the electrode. Thus, dispersion technologies that can facilitate the incorporation of CNT contents as high as possible are critical to achieve optimum battery performances, due to the limited volume of the electrodes. Various methods based on mechanical or chemical routes are available for reducing aggregation and improving the dispersion of CNTs in solvents [46–50].

The main approaches to disperse CNTs using mechanical methods include high-shear mixing [51–57] or ultrasonication [58–62]. The strong mechanical force fragments the CNTs, dispersing them throughout a solvent. However, the fragmented CNTs easily agglomerate after removing the mechanical mixing force, resulting in a short shelf life of the CNT dispersion [63–66]. Other approaches involving chemical agents can effectively resolve the re-agglomeration issues after mechanical dispersion methods [63,67–76]. Chemical approaches are divided in two categories: chemisorption and physisorption methods [77–80]. In the chemisorption methods, the surface of the CNTs is modified or functionalized with various chemical moieties, enhancing the compatibility of the CNTs with a dispersion solvent [81–84]. However, the chemical modification could degrade the electrical properties of the CNTs, because of newly formed defects on their surface or the

* Corresponding author.
E-mail address: bihwang@cau.ac.kr (B. Hwang).

https://doi.org/10.1016/j.colcom.2022.100686
Received 6 September 2022; Received in revised form 18 November 2022; Accepted 12 December 2022
Available online 15 December 2022

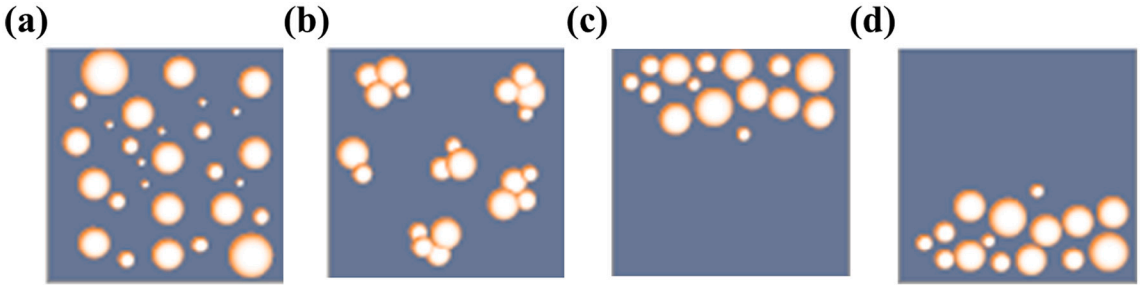

Fig. 1. Schematic illustration of the dispersed states of particles: (a) stable, (b) flocculated or coalesced, (c) creamed, and (d) sedimented.

changed conjugation of π-electrons through the chemical process [85–88]. Physisorption methods modify or functionalize the CNT surface through the physisorption of molecules such as surfactants or polymeric additives which are adsorbed on the CNT surface through π-π interaction or van der Waals forces [88–91]. In physisorption methods, the electrical properties of the CNTs remain unchanged, because the π-electron cloud on the CNT surface is not altered [92–94]. In addition, the physisorption methods are time- and cost-effective; thus, they are widely used for many applications of CNTs, such as nanocomposites or dispersed CNT solutions [85,95–99].

A critical problem in studying CNT dispersions is the accurate evaluation of the dispersion state and stability over time [100]. Slight changes in the dispersion state of CNTs greatly affect the performance of CNT-based batteries; thus, detecting small changes in the dispersion state or stability of one-dimensional nanoscale CNTs is an important task. Several methods have been proposed to measure the dispersion of nanomaterials, such as particle size analysis, UV–vis spectroscopy, zeta potential measurements [101,102], or the detection of transmitted or backscattered light [77,103,104]. Particle size analysis is widely used to evaluate the dispersion state by measuring the size and distribution of CNT agglomerates. A CNT dispersion with uniform size distribution can be considered an indication that the CNTs are well dispersed in the solvent. In case of UV–vis spectroscopy, the absorbance intensity depends on the dispersion state of the CNTs, which enables the characterization of the quality of the dispersion. The zeta potential is a parameter indicating the strength of the repulsive force between adjacent CNTs dispersed in solvents. Thus, a CNT dispersion with a high zeta potential value is considered a stable state. Although these methods can effectively evaluate the dispersion state immediately after dispersion, they may suffer from limitations in the accurate evaluation of the dispersion stability over time. In addition, the above methods require the CNTs to be diluted in a solvent in order to precisely measure their dispersibility; this is another limitation, especially for industries where solutions with high concentrations of CNTs are widely used.

The multiple light scattering is another effective method for measuring the properties of CNT dispersions [77,103,104]. The multiple light scattering can evaluate dispersion properties effectively and precisely, owing to its high-resolution detection and time-dependent measurement ability [65,105–109]. This enables a more reliable evaluation of the dispersion stability. The combined signal of transmitted or backscattered light through samples provides comprehensive information on the dispersion state of samples as a function of the storage time [77,103,104]. Furthermore, unlike methods such as particle size analysis and UV–vis spectroscopy, the multiple light scattering can be applied without any major limitations on the concentration of the particles and the type of solvents. The measurable concentration range is 0.0001–95% (*v*/v). Therefore, a major advantage of the multiple light scattering method is its ability to take samples in their natural (dispersed) state with no dilution or further treatment required. Additionally, the multiple light scattering method can determine dispersion state in highly dilute through highly concentrated colloids. The other methods typically require dilution and are much more time-consuming.

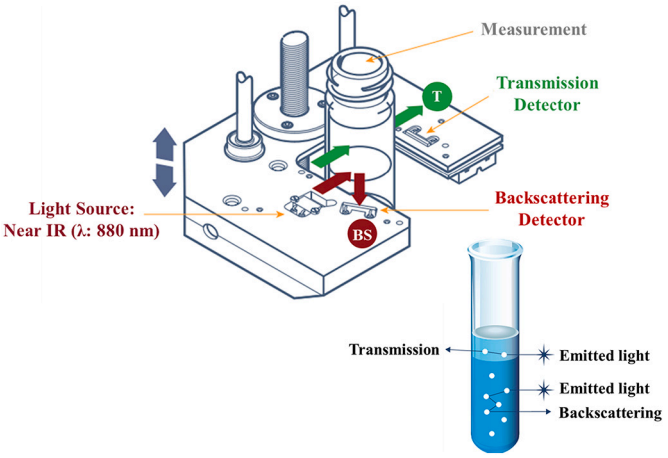

Fig. 2. Schematic illustration of experimental setup for multiple light scattering.

Owing to the importance of investigating CNT dispersions in solution, various studies evaluated the dispersibility of CNTs using the multiple light scattering [64,65,84,107,110–112]. However, a comprehensive review of these studies is still lacking. This mini-review introduces the fundamental theory and mechanism of the multiple light scattering. In addition, various studies on the dispersibility of CNTs using these methods are discussed and summarized. This review provides a comprehensive understanding of the dispersibility of CNTs, especially for systems studied using the multiple light scattering.

1.1. Fundamental principles of multiple light scattering

1.1.1. Mechanisms

Multiple light scattering is an optical measurement method that uses static multiple light scattering to evaluate the stability of a dispersion [113–116]. Slight changes in dispersion states, invisible to the naked eye, can be measured *via* time-dependent *in situ* light detection using a high-precision light detector. The measured data can be used to estimate particle migration parameters and size changes.

The dispersion stability reflects changes in one or more physical characteristics over a certain period; the dispersion state is required information to evaluate the dispersion stability of a sample over time. Dispersion states are divided into four main stages: 1) stable state (Fig. 1(a)), 2) agglomerated state due to flocculation or coalescence (Fig. 1(b)), 3) creamed state (Fig. 1(c)), and 4) sedimented state (Fig. 1(d)). Because the physical or chemical properties of the dispersions are critically governed by their dispersion state, understanding and characterizing the dispersion states of the samples is vital for obtaining stable samples.

Fig. 2 illustrates the multiple light scattering, which typically use a light source capable of irradiating near-infrared rays with a wavelength of 880 nm [117–120]. There are two detectors: a transmission detector

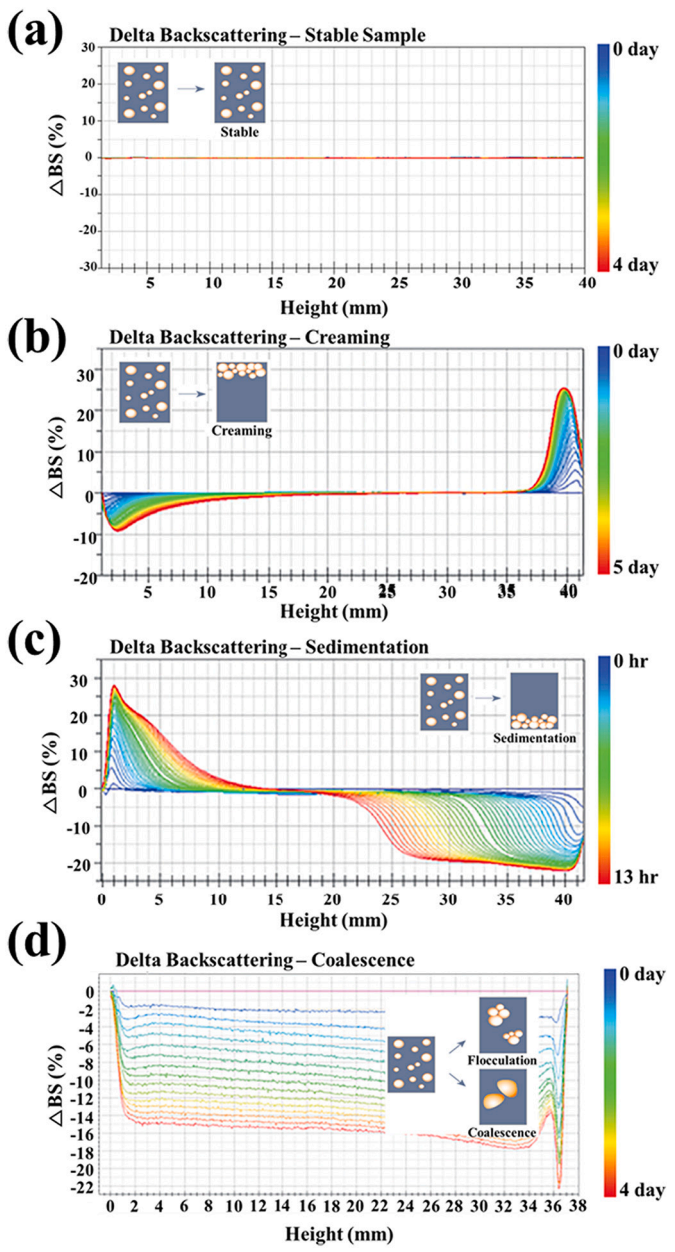

Fig. 3. Illustrations of dispersed particle states and multiple light scattering profiles of (a) stable, (b) creamed, (c) sedimented, and (d) flocculated/coalesced states.

180° opposite the light source and a backscattering detector receiving the light scattered backward, at an angle of 45° from the incident beam. During the characterization process, near-infrared rays are irradiated on the sample and vertically scanned from the sample bottom to the top in 40-μm steps using a pulse method. The detected light source signal at each detector is measured *in situ* during the selected time interval. The irradiated light interacts with the particles in the solution, and the scattering or backscattering of the photons is highly dependent on the angle of the incident light on the particle surface. The light that travels toward the detector on the opposite side of the light source is considered transmitted light, whereas that measured at the detector on the same side of the light source is considered backscattered light. The statistical analysis of the scattered or backscattered light provides valuable information, including the dispersion state, particle size, and sedimentation speed. Therefore, it is practical to characterize time-dependent changes in the dispersion states of samples.

1.1.2. Phenomena in dispersions

Shifts in the transmitted or backscattered light over time are due to changes in the photon transport mean free path, induced by variations in the dispersion state. As shown in the following equations, the photon transport mean free path is determined by the size and concentration of the dispersed particles, resulting in changes in the intensity of the transmitted or backscattered light:

$$\mathrm{BS} \approx \left[\frac{1}{l^*}\right]^{\frac{1}{2}}, T \approx T_0 exp\left[\frac{-r_i}{l}\right], l^* = \left[\frac{2d}{3\Phi(1-g)Q_s}\right], l = \left[\frac{2d}{3\Phi Q_s}\right],$$

where BS denotes backscattering, T_0 represents the transmittance of the continuous phase, g is the asymmetry factor, Q_s is the scattering efficiency factor, d denotes the diameter, Φ represents the concentration, l^* indicates the photon transport mean free path, l is the photon mean free path, and $-r_i$ is the internal radius of the measurement cell [121,122].

Fig. 3 shows representative BS profiles depending on the dispersion states of particles in a solution. The x and y axes correspond to the height of the sample bottle scanned in the measurement and the change in the intensity of the detected backscattered light, respectively. Stable samples exhibit little to no changes in the intensity profile of the measured transmitted or backscattered light (Fig. 3(a)), whereas unstable samples exhibit dramatic changes over time (Fig. 3(b)-3(d)). Aggregation or agglomeration can occur in the unstable samples, altering the particle migration speed or changing the particle size. The degree and path of light scattering show substantial changes through the aggregated particles, which can be easily detected using the multiple light scattering. Particle migration is divided into creaming and sedimentation stages. Creaming is a phenomenon where the particles move upward because their density is lower than that of the solvent. This generates a concentration gradient between the top and bottom of the samples, resulting in local differences between the transmitted and backscattered light (Fig. 3(b)). In the sedimentation case, the particles have higher density than the solvent, resulting in their settling (Fig. 3(c)). The aggregation of particles due to flocculation or coalescence results in an increase in their size, and the inhomogeneous distribution of the particle size causes a variation of the intensity of the transmitted or backscattered light (Fig. 3 (d)); thus, this process can be effectively detected using the multiple light scattering. Flocculation is a process that can be reversed by agitation, whereas coalescence is irreversible.

1.1.3. Factors considered in data analysis

Understanding the effect of concentration and particle size changes is essential to analyze the light detection measurements. The photon transport mean free path is the distance traveled by the photon in a different direction from that of the initially incident light. This is a critical factor determining the intensity of the measured scattered or backscattered light. If the concentration of particles in the bottom region of the cell increases due to sedimentation, without changes in particle size through aggregation, the photon transport mean free path in that region is shortened; this is due to the increased probability of light scattering, which increases the intensity of the backscattered light (Fig. 4(a)). Such concentration of particles in a certain area is termed local concentration. In the opposite case, where the concentration of particles at the bottom of the cell decreases, the photon transport mean free path is extended, reducing the intensity of the backscattered light (Fig. 4(a)). In physical terms, “diluted” and “concentrated” regions can be distinguished based on the intensity of the transmitted light. A concentration corresponding to a 0.2% decrease in the transmitted light intensity is considered a critical concentration, whereas a region with >0.2% decrease is considered a concentrated region. However, in a strongly diluted region, the light reflection at the glass wall of the sample bottle can result in a slight increase in the backscattered light (Fig. 4(b)); this phenomenon is denoted as second wall effect. In other words, the second wall effect corresponds to the increase in intensity caused by the reflection of light by the second wall of the measured cell,

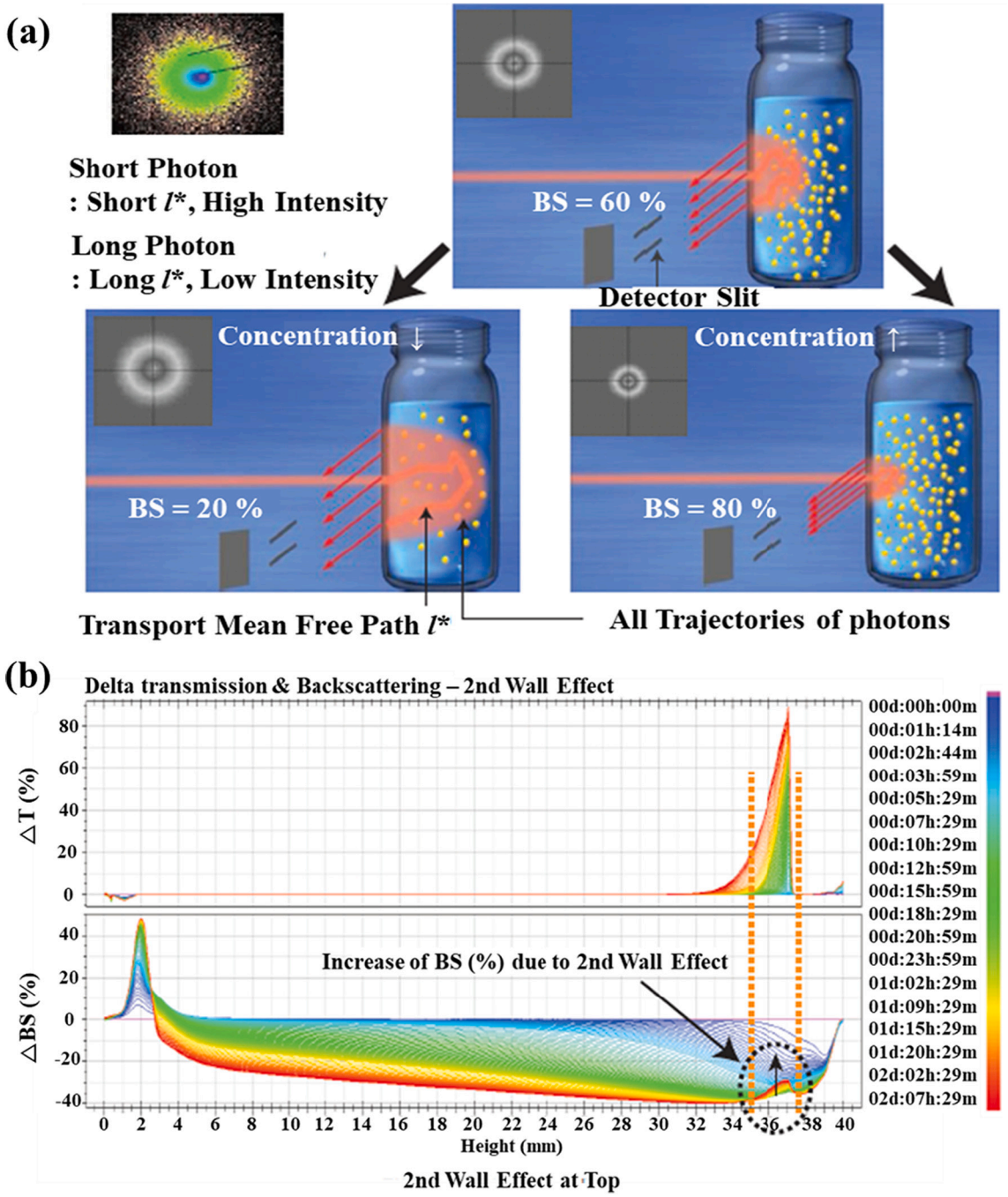

Fig. 4. (a) Schematic illustration of relationships between backscattered light intensity and photon transport mean free path for different particle concentrations; (b) second wall effect of transmission and backscattered light profiles.

rather than scattering by particles dispersed in the solvent; this effect should be considered when analyzing diluted sample results.

Rayleigh and Mie scatterings must be considered in the analysis of particle size changes. Rayleigh scattering, representing elastic scattering at the molecular level, occurs because the particle size is much smaller than the wavelength of the irradiated light (Fig. 5(a)). As the probability of scattering between light and particles is low, the intensity of the backscattered light is also low. As the size of the particles increases due to aggregation over time, the scattering probability between light and particles increases, resulting in an increased backscattering intensity, as illustrated in Fig. 5(c). Mie scattering occurs when the particle size is larger than the wavelength of the irradiated light (Fig. 5(b)). In this region, the average interparticle distance increases with increasing particle size; hence, the probability of scattering decreases, with a gradual decline in the measured intensity of backscattered light (Fig. 5 (c)).

In addition, the optical properties of the particles, such as the refractive index and absorbency, affect the detected intensity of the transmitted or backscattered light. Significant light absorption occurs in highly colored samples; thus, the intensity of the initial backscattered light and the following changes during the measurement are low. Much longer measuring times are required to obtain sensitive results than for samples with other colors.

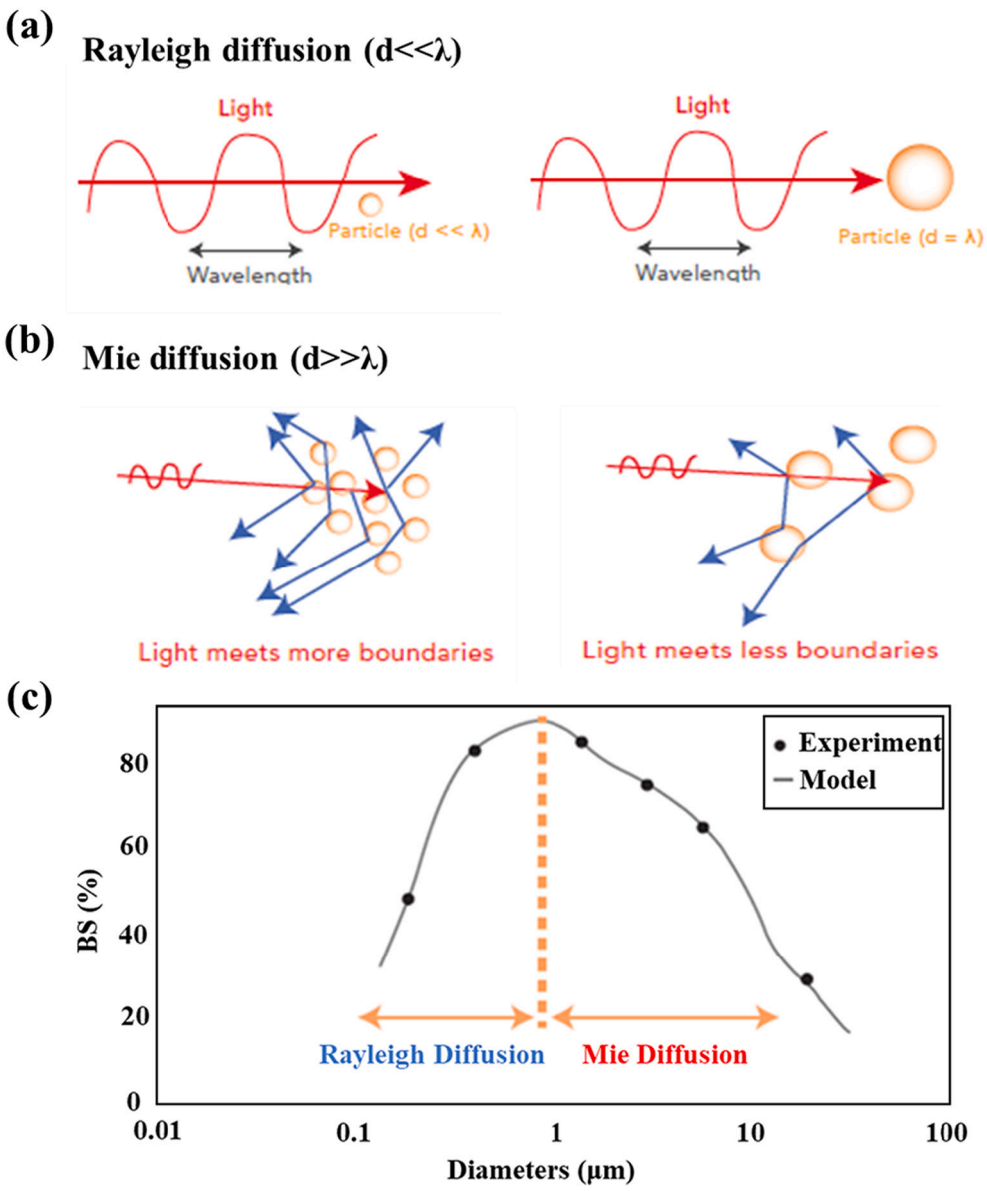

Fig. 5. Illustration of (a) Rayleigh diffusion, (b) Mie diffusion, and (c) changes in backscattered light intensity according to particle size.

1.2. CNT dispersibility studies using multiple light scattering

1.2.1. CNTs dispersed with chemisorption methods

One of the main areas of study among chemical approaches to enhance the stability of CNT dispersions is the functionalization of CNTs using chemisorption methods. Various reports have focused on the dispersion stability of CNTs functionalized with chemisorption methods, which have been intensively studied using multiple light scattering approaches [64,65,84,110,123,124].

Lee et al. [64] compared the dispersion stabilities of three types of MWCNTs: i) pristine MWCNTs, ii) acid-treated MWCNTs with carboxylic acid groups (-COOH), and iii) MWCNTs with carboxyl anion groups (carboxylate, -COO^-). The MWCNTs with different functionalities (0.01 wt%) were dispersed in various nonpolar and polar solvents, including water, styrene, and toluene. The dispersion was performed using a tip sonicator. As shown in Fig. 6(a), the pristine MWCNTs dispersed in water displayed a rapid increase in transmission intensity for up to 1 h, which changed into a gradual increase up to 12 h, indicating significant dispersion instability. Moreover, the MWCNTs-COOH and MWCNTs-COO^- dispersions in water presented no significant changes in transmission signals even after 12 h, indicating dispersion stability. The sedimentation of the MWCNTs-COO^- dispersion was slower than that of the MWCNTs-COOH counterpart, owing to the stronger electrostatic repulsion forces between MWCNTs-COO^- species [64,119,125].

As illustrated in Fig. 6(b), polar solvents (*i.e.*, water) were found to be a little more beneficial for the dispersion stability of pristine MWCNTs compared to nonpolar solvents, such as styrene or toluene. For MWCNTs-COO^-, the dispersion in polar solvents, such as methanol or water, exhibited much higher stability than that in styrene (Fig. 6(c)). Polar carboxylic anions groups (-COO^-) resulted in strong electrostatic repulsion forces between MWCNTs-COO^- species, especially in polar solvents, leading to a greater dispersion stability in polar than nonpolar solvents. These findings indicated that the surface functionalization of MWCNTs to introduce strong electrostatic repulsion is an effective route for achieving dispersion stability in polar solvents; however, further efforts are required to enhance the dispersion stability in nonpolar solvents.

Kim et al. [124] synthesized MWCNTs with long-chain alkyl groups produced by alkylation of carboxylate sodium salts (Fig. 7(a)). A 0.05 wt % amount of the fabricated MWCNTs with carboxyl ester alkyl groups

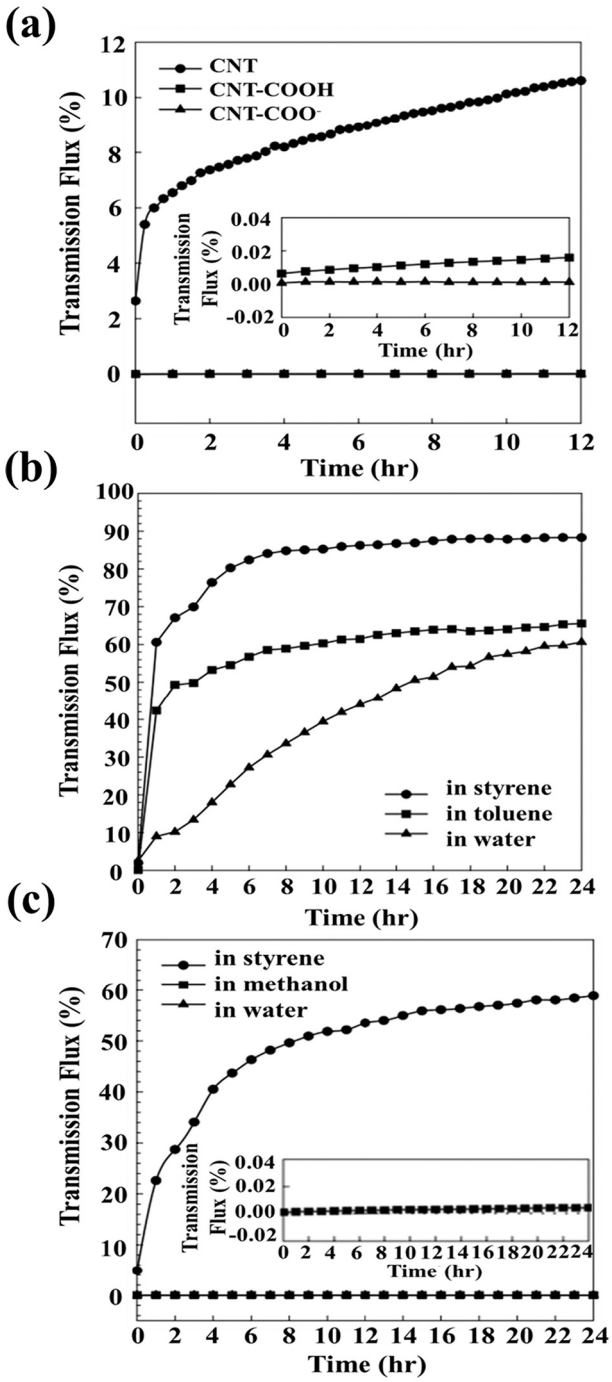

Fig. 6. (a) Transmission profiles of pristine MWCNTs, MWCNTs-COOH, and MWCNTs-COO^- dispersed in water. (b) Transmission profiles of pristine MWCNTs dispersed in styrene, toluene, and water. (c) Transmission profiles of MWCNTs-COO^- dispersed in styrene, methanol, and water. Reproduced with permission from [64].

was dispersed in toluene by ultrasonication for 4 h. The authors measured the stability of the alkylated MWCNTs hourly for 10 days. The alkylated MWCNTs displayed much higher dispersion stability than the pristine MWCNTs even after 10 days of measurements, because the long alkyl chains enhanced the solubility of the MWCNTs in the solvents and prevented their aggregation (Fig. 7(b)).

Wang et al. [110] synthesized MWCNTs grafted with an amphiphilic block copolymer *via* covalent bonds to achieve high MWCNT dispersion stability in various solvents. Poly(*tert*-butyl methylacrylate) (PtBMA)

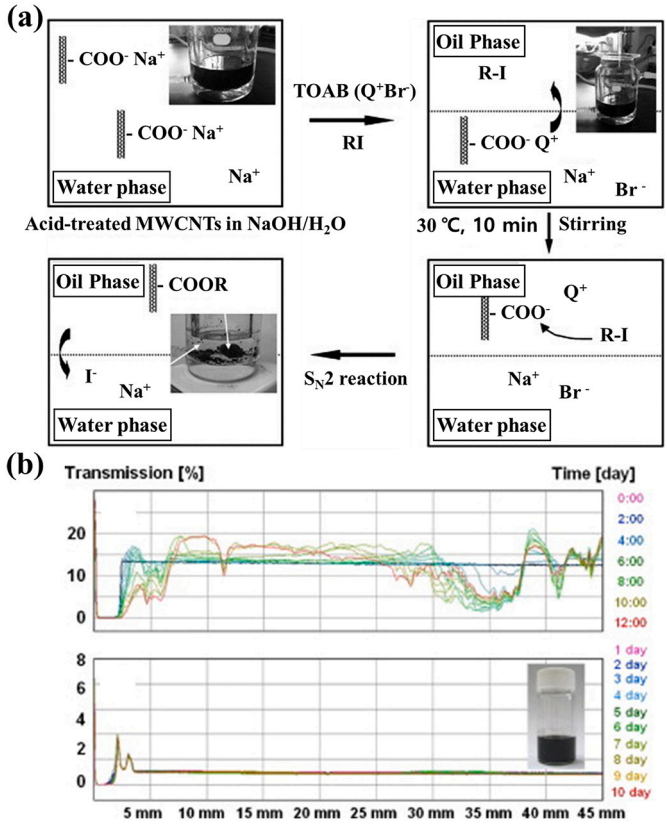

Fig. 7. (a) Fabrication procedure of alkylated MWCNTs and (b) transmitted light profiles of pristine and alkylated MWCNTs in toluene. Reproduced with permission from [124].

was reacted with polystyrene (PSt) to produce a block copolymer, which then reacted with MWCNTs *via* azide coupling to form PtBMA-*b*-PSt-MWCNTs (Sample C) (Fig. 8(a)). The hydrolysis of PtBMA-*b*-PSt-MWCNTs converted PtBMA to a polymethylacrylic acid (PMAA) block, which produced PMAA-*b*-PSt-MWCNTs (Sample B) (Fig. 8(a)). 0.05 wt% amount of MWCNTs with various functionalities were dispersed in various hydrophilic (*e.g.*, water and ethanol) and hydrophobic (*e.g.*, acetone and chloroform) solvents. The dispersion was performed using a sonicator for 2 min.

Samples B and C presented a much better sedimentation behavior than pristine MWCNTs (Fig. 9(b– e)), indicating that functionalization using block copolymers is an effective method to enhance the sedimentation stability of CNTs. In comparison, Sample C exhibited a better sedimentation behavior than Sample B (Fig. 9(b–e)). The PMAA chain with carboxyl functional groups (-COOH) in Sample B resulted in a larger average size of the entangled MWCNTs, accelerating the sedimentation [110,126,127]. Consequently, the block copolymer without -COOH functional groups is beneficial to achieve a high dispersion stability.

1.2.2. CNTs dispersed with physisorption methods

As discussed in section 2.2.1, the chemisorption methods effectively enhanced the CNT dispersion stability. However, the generated surface defects on the CNT surface might degrade the electrical properties of the CNTs, which can in turn reduce the performance of devices based on them [86,91,101,128–130]. In addition, the functionalization process is relatively toxic and complicated. Thus, physisorption methods are the preferred option to enhance the stability of CNT dispersions. The precise characterization of the stability of CNTs dispersed using physisorption methods is also critical; thus, many studies have investigated the stability of CNT dispersions using physisorption and multiple light

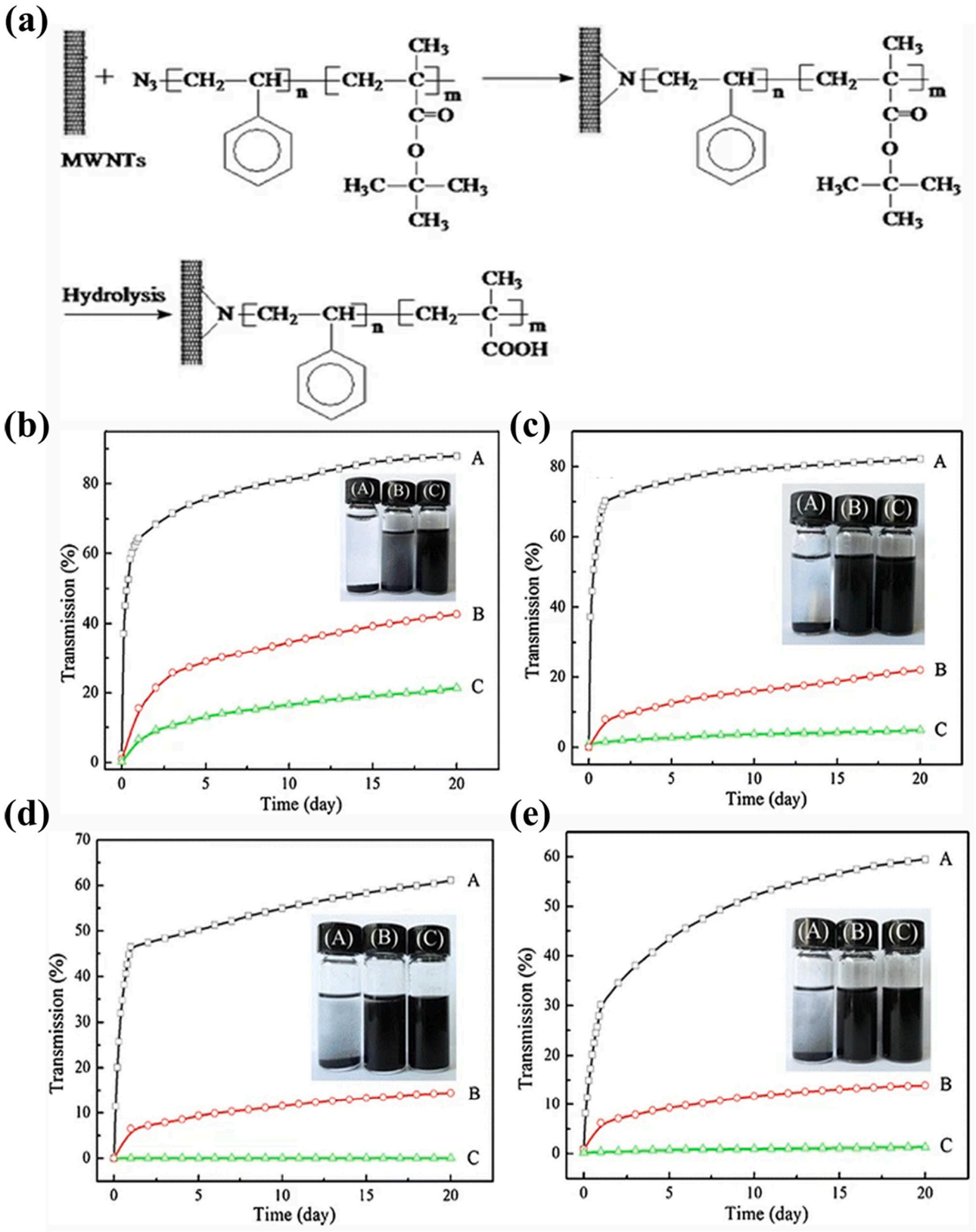

Fig. 8. (a) Schematic diagram of the synthesis of PMAA-*b*-PSt-MWCNTs; (b–e) transmission profiles of A: pristine MWCNTs, B: PMAA-*b*-PSt-MWCNTs, and C: PtBMA-*b*-PSt-MWCNTs dispersed in (b) water, (c) ethanol, (d) acetone, and (e) chloroform. Reproduced with permission from [110].

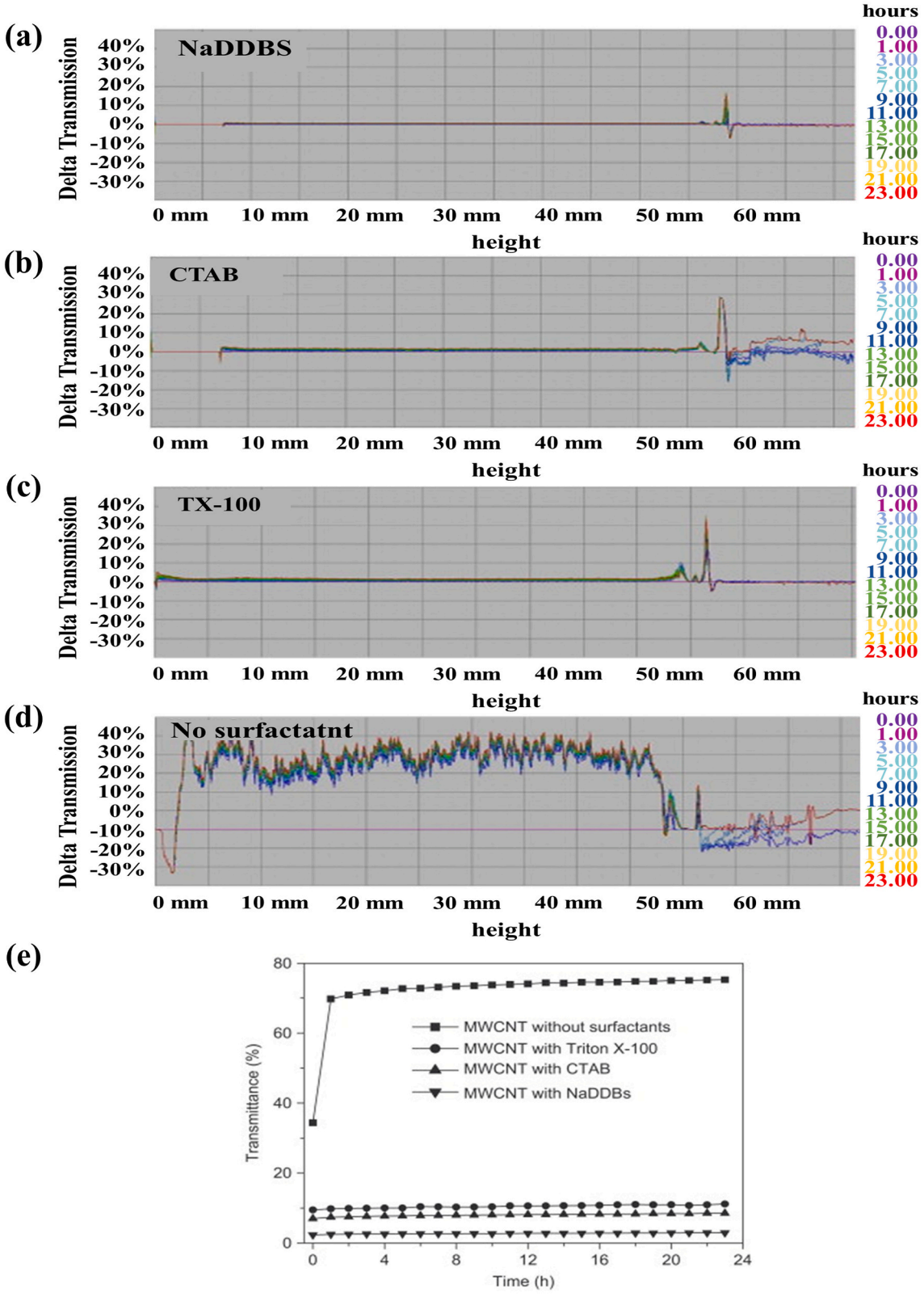

Fig. 9. Transmission profiles of MWCNTs dispersed in water with (a) NaDDBS, (b) CTAB, (c) TX-100, and (d) no surfactants. (e) Comparison of transmittances of MWCNTs dispersed with different surfactants. Reproduced with permission from [107].

scattering.

Kim et al. [107] dispersed MWCNTs in water and compared the stability of the dispersions using multiple light scattering. Various surfactants, such as sodium dodecylbenzene sulfonate (NaDDBS) as anionic surfactant, cetyltrimethylammonium bromide (CTAB) as cationic surfactant, and nonionic Triton-X-100 were used to disperse the MWCNTs. 0.3 wt% of surfactants and 0.02 wt% of MWCNTs were mixed in water and sonicated at 25 °C at a power of 600 W and 28 kHz for 7 h. The

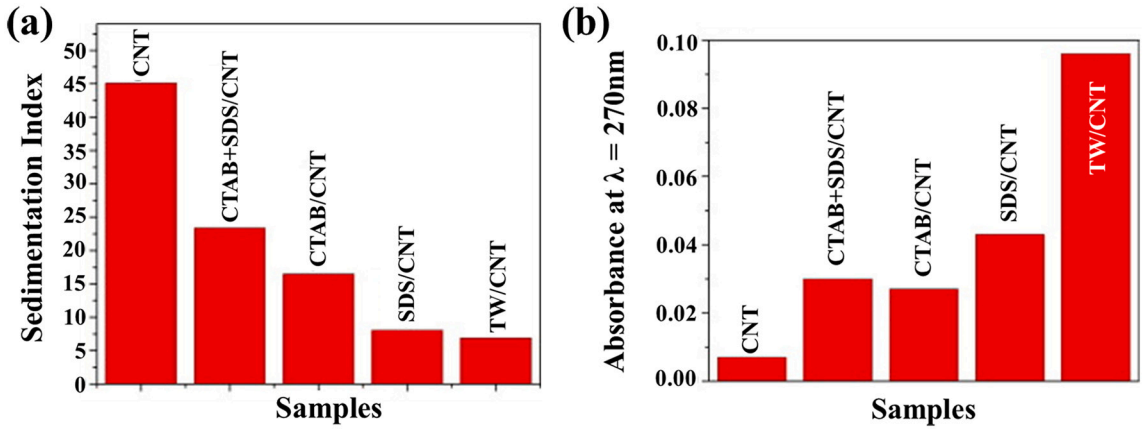

Fig. 10. (a) Sedimentation index and (b) absorbance intensity (at a wavelength of 270 nm) of MWCNTs dispersed in water using various surfactants. Reproduced with permission from [131].

authors analyzed the transmittance of each sample for 24 h at time intervals of 1 h. All surfactants were effective in enhancing the dispersion stability of the MWCNTs, and the sedimentation of MWCNTs dispersed with surfactants was much lower than that of pristine MWCNTs (Fig. 10 (a–d)). Among the various surfactants, NaDDBS (anionic surfactant) was the most effective for MWCNT dispersion in water, due to strong electrostatic repulsion (Fig. 10(e)).

Ponnamma et al. [131] studied MWCNTs dispersed in water using ionic surfactants with different surface charges, such as sodium dodecyl sulfate (SDS) and CTAB, as well as with a nonionic surfactant, Tween 20 (TW). The dispersion stability of MWCNTs dispersed with different surfactants was systematically studied by detecting the amount of transmitted and backscattered light signals through sample bottles. The content of MWCNTs in the solvent was 0.1 wt%, which was then diluted by 100 times. The dispersion was performed using a bath sonicator for 3 h, followed by magnetic stirring for 36 h at room temperature. The ratio of surfactants to MWCNTs was fixed at 5:1. To evaluate the sedimentation stability, the results were presented in terms of sedimentation indexes (Fig. 11), with a lower index indicating higher sedimentation and dispersion stabilities. The pristine MWCNTs had the highest sedimentation index. Use of CTAB and SDS reduced the sedimentation index, but the different charges of the cationic CTAB and anionic SDS caused the aggregation of the MWCNTs, when used in mixtures, resulting in relatively poorer stability compared to MWCNTs with a single

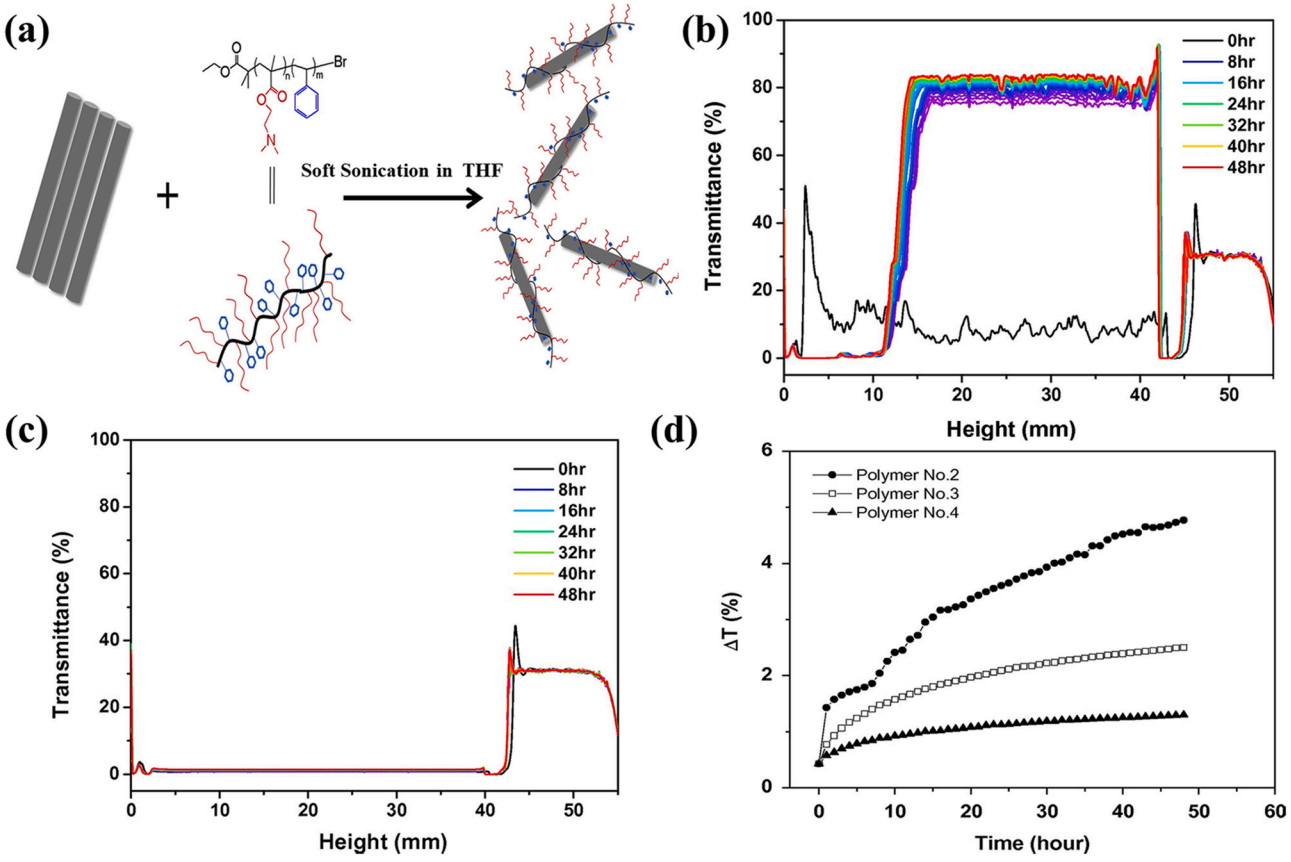

Fig. 11. (a) Fabrication of SWCNTs with poly(DMAEMA-*co*-St) in THF. Transmission profiles of (b) pristine SWCNTs and (c) SWCNTs with poly(DMAEMA-*co*-St) in THF; (d) comparison of transmittances of SWCNT dispersions with different DMAEMA/St ratios. Reproduced with permission from [111].

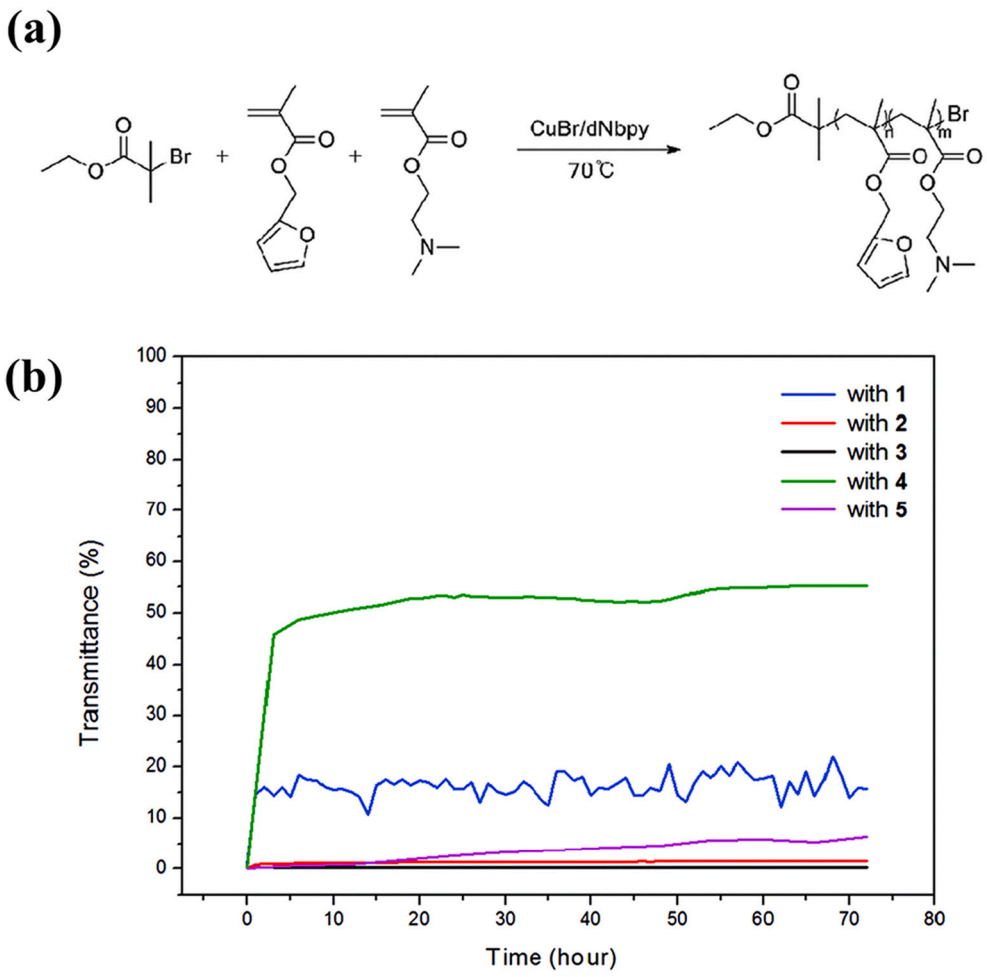

Fig. 12. (a) Synthesis procedure of p(FMA-*co*-DMAEMA) polymeric dispersant. (b) Transmittance changes of SWCNTs in THF, depending on the ratio of FMA to DMAEMA. Reproduced with permission from [112].

surfactant. The cationic CTAB and the electrons of MWCNTs neutralized the surface charge, resulting in a higher stability compared with MWCNTs with CTAB and SDS. The anionic SDS or nonionic TW presented similar excellent dispersion stabilities, maintaining a negative charge on the MWCNT surface. These results indicated that the charge of the surfactant is a critical property for achieving high dispersion stability. In addition, the enhanced performance of TW is related to efficiency of binding of head group to CNT surface, where the molecular structure of TW is large and very efficient at binding. TW is a nonionic surfactant, with long hydrocarbon chains compared to SDS and CTAB. Thus, it does not disrupt the natural negative surface charge of CNT as it is a non-ionic surfactant. Therefore, TW would be stabilizer that operates both sterically and electrostatically, which resulted in the high sedimentation stability. Furthermore, depending on the types of surfactants, they also measured the UV–vis spectra of 0.1 wt% MWCNT dispersions with a further 1000 times dilution. They plotted the UV–vis absorption intensity at a wavelength of ~270 nm, because the high absorbance in the range of the 200–300 nm is one of the ways to measure the stability of well-dispersed CNTs [132]. Similar to the trends of the sedimentation index, the MWCNT dispersion with TW showed the highest absorbance, whereas the MWCNT dispersion without surfactant showed the lowest absorbance compared with other cases. These results also prove that adjusting the surfactant is an essential way to improve the stability of MWCNT dispersions.

Kim et al. [111] investigated the dispersion stability of single-walled CNTs (SWCNTs) with a polymeric dispersant using the multiple light scattering. In this study, 3 mg of SWCNTs was dispersed in 20 mL of tetrahydrofuran (THF) with 30 mg of poly(2-dimethylamino)ethyl methacrylate-*co*-styrene (poly(DMAEMA-*co*-St) as a polymeric dispersant (Fig. 12(a)). The dispersion was conducted using a bath-type sonicator for 3 h. To evaluate the sedimentation stability, the authors plotted the transmittance results by measuring 48 scans for 2 days. The polymeric dispersants were synthesized by controlling the monomer ratio of DMAEMA to St. The aromatic groups of St interacted with SWCNTs *via* physisorption π-π interactions. In addition, DMAEMA created a steric hindrance between the individual SWCNTs. Therefore, the combination of St and DMAEMA was effective in preventing SWCNT aggregation, enhancing the dispersion stability (Fig. 12(b) and 12(c)). The dispersant prepared with a DMAEMA/St mixing ratio of 7:3 (No. 4) exhibited the highest sedimentation stability, as illustrated in Fig. 12(d). Samples No. 2 and No. 3 were synthesized with DMAEMA/St mixing ratios of 20:80 and 46:54, respectively. The role of St in the mixture was to promote the adhesion of DMAEMA to the CNT surface. The dispersion stability was mainly due to the steric hindrance produced by DMAEMA. Therefore, increasing the content of DMAEMA resulted in better performances. However, DMAEMA alone (without St) showed the worst dispersibility, because it is impossible to anchor it on the CNT surface without St. Therefore, mixing DAMEMA and St was necessary to obtain the best dispersibility of the CNT solution. The St or DMAEMA single components displayed much faster sedimentation than the mixed samples. These results indicated that the mixture of St and DMAEMA improves the dispersion stability of SWCNTs in THF.

Lee et al. [112] dispersed SWCNTs in THF with poly((furfuryl methacrylate)-*co*-(2-(dimethylamino)ethyl methacrylate)) (p(FMA-*co*-

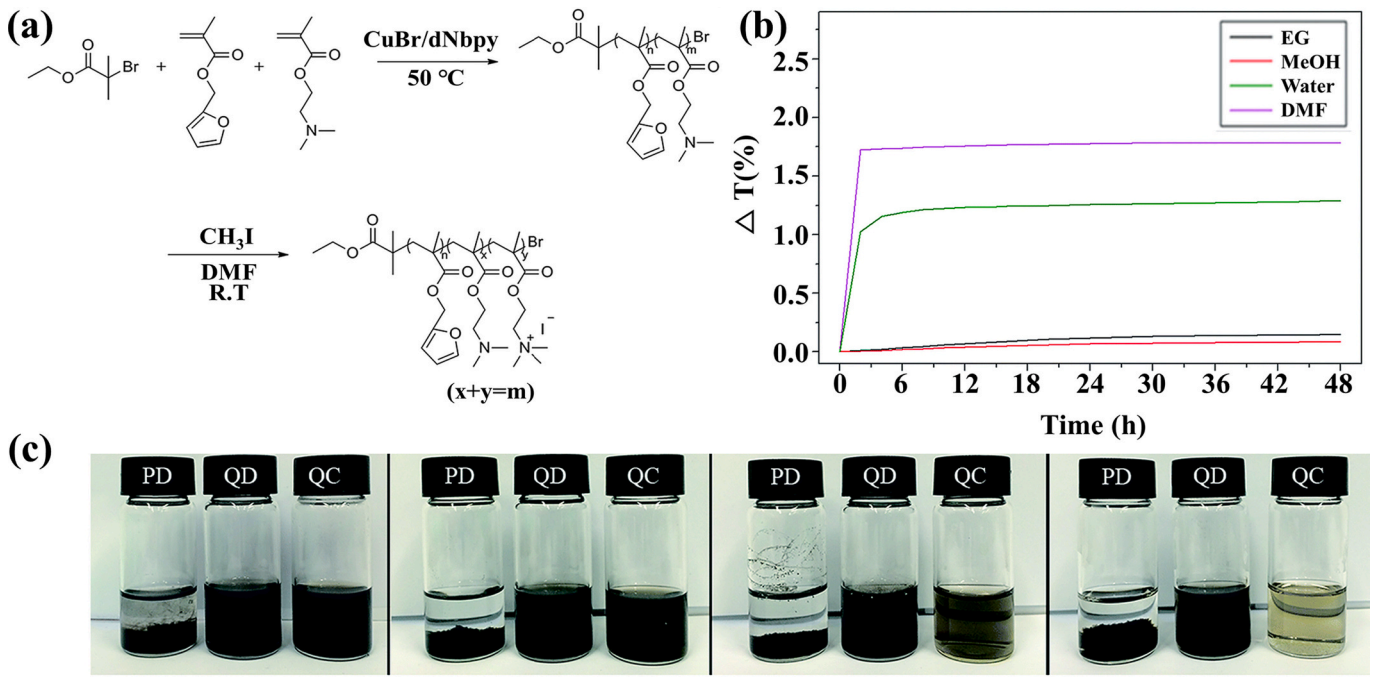

Fig. 13. (a) Schematic illustration of the fabrication procedure of p(FMA-*co*-QDMAEMA). (b) Transmittance data for SWCNTs dispersed with p(FMA-*co*-QDMAEMA) in various solvents. (c) Optical images of SWCNT dispersions in EG, MeOH, water, and DMF (PD: SWCNT dispersion with p(FMA-*co*-DMAEMA), QD: SWCNT dispersion with p(FMA-*co*-QDMAEMA), QC: centrifuged QD solution). Reproduced with permission from [133].

Table 1
Summary of various strategies to enhance CNT dispersion stability.

Modification method		CNT	Solvent	Dispersion method	Dispersion stability	Ref.
Chemisorption method	Acid treatment	0.03 wt% of MWCNTs	Methanol Ethanol Isopropanol	Ultrasonication for 8 h	Excellent Excellent Excellent	[65]
	Acid treatment and anionization of carboxylic acid group	0.01 wt% of MWCNTs	Styrene Methanol Water	Tip sonication	Poor Excellent Excellent	[64]
	Alkylation	0.05 wt% of MWCNTs	Toluene	Ultrasound sonication for 4 h	Excellent	[124]
	Amphiphilic block copolymer modification	0.05 wt% of MWCNTs	Water Ethanol Acetone Chloroform	Sonication for 2 min	Fair Excellent Excellent Excellent	[110]
Physisorption method	0.3 wt% of NaDDBS 0.3 wt% of CTAB 0.3 wt% of Triton-X-100	0.02 wt% of MWCNTs	Water	Sonication at 600 W power and 28 kHz for 7 h	Excellent Excellent Excellent	[107]
	0.005 wt% of TW 0.005 wt% of SDS 0.005 wt% of CTAB 0.005 wt% of CTAB + SDS	0.001 wt% of MWCNTs	Water	Bath-type sonication for 3 h followed by magnetic stirring for 36 h	Excellent Excellent Fair Fair	[131]
	0.17 wt% of poly(DMAEMA-*co*-St)	0.017 wt% of SWCNTs	THF	Bath-type sonication for 3 h	Excellent	[111]
	0.11 wt% of poly(FMA-*co*-DMAEMA)	0.011 wt% of SWCNTs	THF	Bath-type sonication for 3 h	Excellent	[112]
	0.09 wt% of poly(FMA-*co*-QDMAEMA)	0.009 wt% of SWCNTs	EG	Bath-type sonication for 3 h	Excellent	[133]
	0.12 wt% of poly(FMA-*co*-QDMAEMA)	0.012 wt% of SWCNTs	MeOH		Excellent	
	0.1 wt% of poly(FMA-*co*-QDMAEMA)	0.01 wt% of SWCNTs	Water		Excellent	
	0.11 wt% of poly(FMA-*co*-QDMAEMA)	0.011 wt% of SWCNTs	DMF		Excellent	

DMAEMA)) as a polymeric dispersant (Fig. 13(a)). 2 mg of SWCNTs was mixed with 20 mL of THF and the resulting solution was mixed with 20 mg of the polymeric dispersant using a bath sonicator for 3 h. The ratio of FMA to DMAEMA was varied from 1:0, to 7:3, 5:5, 3:7, and 0:1, and the corresponding samples were labeled 1, 2, 3, 4, and 5, respectively. However, a critical range of mixing ratios exhibited optimized SWCNT sedimentation behavior in THF. The 7:3 (2) and 5:5 (3) FMA/DMAEMA mixing ratios led to excellent sedimentation behavior, as shown in Fig. 13(b). A further increase in DMAEMA content to 70% (4) resulted in a rapid deterioration of the sedimentation performance, as shown in

Fig. 13b, due to fast phase separation.

Lee et al. [133] also reported the enhanced dispersibility of SWCNTs using modified p(FMA-*co*-DMAEMA). The tertiary amine p(FMA-*co*-DMAEMA) was modified to quaternary ammonium (p(FMA-*co*-QDMAEMA)) using iodomethane, as illustrated in Fig. 14(a). The p(FMA-*co*-QDMAEMA) compound had a positive charge center, making the SWCNTs soluble in ethylene glycol (EG), dimethylformamide (DMF), water, and methanol (MeOH). 4 mg of SWCNTs was dispersed in 40 mL of solvent along with 40 mg of the dispersants, using a bath sonicator for 3 h. Changes in the transmitted light through the sample bottles were measured using the multiple light scattering for 2 days at time intervals of 2 h. The SWCNTs dispersed with p(FMA-*co*-QDMAEMA) displayed excellent sedimentation behavior, with a transmittance change below 2% over 2 days (Fig. 14(b)). The SWCNTs with the unmodified dispersant (p(FMA-*co*-DMAEMA)) exhibited poor sedimentation in EG, MeOH, water, and DMF systems (Fig. 14(c)). These results indicate that the modification of the polymeric dispersant is another suitable strategy to further enhance the sedimentation stability of SWCNTs.

Table 1 summarizes the literature described in section 2.2 of this mini-review; the different studies are classified according to modification method, CNT content, type of solvent, mixing method, and dispersion stability evaluated from the characterization results using the multiple light scattering. Overall, the dispersibility of dispersions of various CNTs and additives was successfully characterized using the multiple light scattering. The dispersibility of CNTs was mainly determined by the modification method and solvent; thus, selecting appropriate chemicals that are effective to the target solvent system was shown to be crucial to obtain highly stable CNT dispersions.

2. Summary

This mini-review discusses the trends observed in CNT dispersibility studies using the multiple light scattering. The initial part of the review described the operation mechanism of the method and the factors considered in the data analysis. This light detection method rapidly and accurately measures the dispersion stability of complex dispersed samples such as CNT samples by detecting changes in backscattered and transmitted light According to the literature results described in this mini-review, physisorption methods are relatively easier to apply than chemisorption methods. The dispersion stability was highly dependent on the interaction between the CNT surface and the solvent; thus, different strategies will be required to achieve an optimized dispersion stability of CNTs with different solvents. Although this mini-review provides some indications of the strategies that could be used for CNT dispersion, there are many unexplored materials or methods that can further enhance the dispersion stability of CNTs. In addition, the relation between the dispersion stability of CNTs and the performance of batteries has not been intensively studied yet. Owing to its ability to precisely detect dispersion states *in situ*, the transmitted and backscattered light detection method is expected to support future studies aimed to enhance the CNT dispersion stability, especially in secondary battery applications.

Funding

Byungil Hwang acknowledges financial support from the National Research Foundation of Korea (NRF-2022R1F1A1063696 and 2019K1A3A1A25000230).

Availability of data and materials

Not applicable.

Ethics approval and consent to participate

Not applicable.

Consent for publication

Not applicable.

Declaration of Competing Interest

The authors have no relevant financial or nonfinancial interests to disclose.

Data availability

The authors do not have permission to share data.

Acknowledgment

The authors acknowledge technical support from Lean on Tech (Korea), especially for the preparation of Figs. 1–5.

References

[1] Y. Song, H. Chen, Z. Su, X. Chen, L. Miao, J. Zhang, X. Cheng, H. Zhang, Highly compressible integrated supercapacitor–piezoresistance-sensor system with CNT–PDMS sponge for health monitoring, small 13 (39) (2017) 1702091.
[2] Z. Zhang, Y. Zhang, X. Jiang, H. Bukhari, Z. Zhang, W. Han, E. Xie, Simple and efficient pressure sensor based on PDMS wrapped CNT arrays, Carbon 155 (2019) 71–76.
[3] H.-R. Lim, Y. Lee, K.A. Jones, Y.-T. Kwon, S. Kwon, M. Mahmood, S.M. Lee, W.-H. Yeo, All-in-one, wireless, fully flexible sodium sensor system with integrated Au/CNT/Au nanocomposites, Sensors Actuators B Chem. 331 (2021), 129416.
[4] B. Hwang, Y. Han, P. Matteini, Bending fatigue behavior of ag nanowire/cu thin-film hybrid interconnects for wearable electronics, Facta Univ. Ser.: Mech. Eng. 20 (3) (2022) 553–560.
[5] N.A. Demidenko, A.V. Kuksin, V.V. Molodykh, E.S. Pyankov, L.P. Ichkitidze, V. A. Zaborova, A.A. Tsymbal, S.A. Tkachenko, H. Shafaei, E. Diachkova, Flexible strain-sensitive silicone-CNT sensor for human motion detection, Bioengineering 9 (1) (2022) 36.
[6] N. Anjum, J.-H. He, Q.T. Ain, D. Tian, Li-he's modified homotopy perturbation method for doubly-clamped electrically actuated microbeams-based microelectromechanical system, Facta Univ. Ser.: Mech. Eng. 19 (4) (2021) 601–612.
[7] E. Willert, Fft-based implementation of the mdr transformations for homogeneous and power-law graded materials, Facta Univ. Ser.: Mech. Eng. 19 (4) (2021) 805–816.
[8] D. Chaudhary, S. Munjal, N. Khare, V. Vankar, Bipolar resistive switching and nonvolatile memory effect in poly (3-hexylthiophene)–carbon nanotube composite films, Carbon 130 (2018) 553–558.
[9] J. Sánchez-Vásquez, B. Portillo-Rodríguez, E. Tovar-Martínez, M. Reyes-Reyes, R. López-Sandoval, Resistive organic memory devices based on nitrogen-doped CNTs/PSS composites, J. Mater. Sci. Mater. Electron. (2022) 1–17.
[10] F.N. Molinari, E. Barragán, E. Bilbao, L. Patrone, G. Giménez, A.V. Medrano, A. Tolley, L.N. Monsalve, An electrospun polymer composite with fullerene-multiwalled carbon nanotube exohedral complexes can act as memory device, Polymer 194 (2020), 122380.
[11] E. Zhao, X. Liu, G. Liu, B. Zhou, C. Xing, Rewritable bistable memory device in polymethyl methacrylate carbon nanotube composite films, J. Mater. Sci. Mater. Electron. 31 (4) (2020) 3642–3647.
[12] I. Sanchez Esqueda, X. Yan, C. Rutherglen, A. Kane, T. Cain, P. Marsh, Q. Liu, K. Galatsis, H. Wang, C. Zhou, Aligned carbon nanotube synaptic transistors for large-scale neuromorphic computing, ACS Nano 12 (7) (2018) 7352–7361.
[13] D. Pamučar, M. Žižović, S. Biswas, D. Božanić, A new logarithm methodology of additive weights (lmaw) for multi-criteria decision-making: Application in logistics, Facta Univ. Ser.: Mech. Eng. 19 (3) (2021) 361–380.
[14] H. Hao, D. Hui, D. Lau, Material advancement in technological development for the 5G wireless communications, Nanotechnol. Rev. 9 (1) (2020) 683–699.
[15] A. Koochi, M. Goharimanesh, Nonlinear oscillations of cnt nano-resonator based on nonlocal elasticity: The energy balance method, Rep. Mech. Eng. 2 (1) (2021) 41–50.
[16] P.M. Grubb, F. Bidoky, A. Mahajan, H. Subbaraman, W. Li, D. Frisbie, R.T. Chen, X-band printed phased array antennas using high-performance CNT/ion gel/Ag transistors, in: Laser 3D Manufacturing III, SPIE, 2016, pp. 162–173.
[17] E. Amram Bengio, D. Senic, L.W. Taylor, R.J. Headrick, M. King, P. Chen, C. A. Little, J. Ladbury, C.J. Long, C.L. Holloway, Carbon nanotube thin film patch antennas for wireless communications, Appl. Phys. Lett. 114 (20) (2019), 203102.
[18] J.-H. He, W.-F. Hou, N. Qie, K.A. Gepreel, A.H. Shirazi, H.M.-. Sedighi, Hamiltonian-based frequency-amplitude formulation for nonlinear oscillators, Facta Univ. Ser.: Mech. Eng. 19 (2) (2021) 199–208.
[19] M. Popov, Friction under large-amplitude normal oscillations, Facta Univ. Ser.: Mech. Eng. 19 (1) (2021) 105–113.

[20] X.-M. Liu, Z. Dong Huang, S. Woon Oh, B. Zhang, P.-C. Ma, M.M. Yuen, J.-K. Kim, Carbon nanotube (CNT)-based composites as electrode material for rechargeable Li-ion batteries: a review, Compos. Sci. Technol. 72 (2) (2012) 121–144.

[21] W. Yuan, Y. Zhang, L. Cheng, H. Wu, L. Zheng, D. Zhao, The applications of carbon nanotubes and graphene in advanced rechargeable lithium batteries, J. Mater. Chem. A 4 (23) (2016) 8932–8951.

[22] S. Sun, Q. Yan, M. Wu, X. Zhao, Carbon aerogel based materials for secondary batteries, Sustain. Mater. Technol. 30 (2021), e00342.

[23] A.L.M. Reddy, M.M. Shaijumon, S.R. Gowda, P.M. Ajayan, Coaxial MnO2/carbon nanotube array electrodes for high-performance lithium batteries, Nano Lett. 9 (3) (2009) 1002–1006.

[24] S. Szalai, S.K. Szürke, D. Harangozó, S. Fischer, *Investigation of deformations of a lithium polymer cell using the digital image correlation method (dicm)*, Rep. Mech. Eng. 3 (1) (2022) 116–134.

[25] E. Nossol, V.H. Souza, A.J. Zarbin, Carbon nanotube/Prussian blue thin films as cathodes for flexible, transparent and ITO-free potassium secondary battery, J. Colloid Interface Sci. 478 (2016) 107–116.

[26] L. Liu, M. Cheng, Z. Yang, Improved performance of flower-like ZnAl LDH growing on carbon nanotubes used in zinc–nickel secondary battery, Electrochim. Acta 277 (2018) 67–76.

[27] T. Kim, Y. Mo, K. Nahm, S.M. Oh, Carbon nanotubes (CNTs) as a buffer layer in silicon/CNTs composite electrodes for lithium secondary batteries, J. Power Sources 162 (2) (2006) 1275–1281.

[28] S.W. Lee, N. Yabuuchi, B.M. Gallant, S. Chen, B.-S. Kim, P.T. Hammond, Y. Shao-Horn, High-power lithium batteries from functionalized carbon-nanotube electrodes, Nat. Nanotechnol. 5 (7) (2010) 531–537.

[29] Y. Luo, K. Wang, Q. Li, S. Fan, J. Wang, Macroscopic carbon nanotube structures for lithium batteries, Small 16 (15) (2020) 1902719.

[30] Z. Wu, K. Liu, C. Lv, S. Zhong, Q. Wang, T. Liu, X. Liu, Y. Yin, Y. Hu, D. Wei, Ultrahigh-energy density lithium-ion cable battery based on the carbon-nanotube woven macrofilms, Small 14 (22) (2018) 1800414.

[31] J.H. Lee, C.S. Yoon, J.-Y. Hwang, S.-J. Kim, F. Maglia, P. Lamp, S.-T. Myung, Y.-K. Sun, High-energy-density lithium-ion battery using a carbon-nanotube–Si composite anode and a compositionally graded Li [Ni 0.85 Co 0.05 Mn 0.10] O 2 cathode, Energy Environ. Sci. 9 (6) (2016) 2152–2158.

[32] L. Zhu, W. Zhu, X.-B. Cheng, J.-Q. Huang, H.-J. Peng, S.-H. Yang, Q. Zhang, Cathode materials based on carbon nanotubes for high-energy-density lithium–sulfur batteries, Carbon 75 (2014) 161–168.

[33] J.W. Hu, Z.P. Wu, S.W. Zhong, W.B. Zhang, S. Suresh, A. Mehta, N. Koratkar, Folding insensitive, high energy density lithium-ion battery featuring carbon nanotube current collectors, Carbon 87 (2015) 292–298.

[34] B.J. Landi, C.D. Cress, R.P. Raffaelle, High energy density lithium-ion batteries with carbon nanotube anodes, J. Mater. Res. 25 (8) (2010) 1636–1644.

[35] V. Popov, Energetic criterion for adhesion in viscoelastic contacts with non-entropic surface interaction, Rep. Mech. Eng. 2 (1) (2021) 57–64.

[36] W. Weng, H. Lin, X. Chen, J. Ren, Z. Zhang, L. Qiu, G. Guan, H. Peng, Flexible and stable lithium ion batteries based on three-dimensional aligned carbon nanotube/silicon hybrid electrodes, J. Mater. Chem. A 2 (24) (2014) 9306–9312.

[37] J. Mun, J.-H. Park, W. Choi, A. Benayad, J.-H. Park, J.-M. Lee, S.-G. Doo, S.M. Oh, New dry carbon nanotube coating of over-lithiated layered oxide cathode for lithium ion batteries, J. Mater. Chem. A 2 (46) (2014) 19670–19677.

[38] K. Wang, Y. Wu, S. Luo, X. He, J. Wang, K. Jiang, S. Fan, Hybrid super-aligned carbon nanotube/carbon black conductive networks: a strategy to improve both electrical conductivity and capacity for lithium ion batteries, J. Power Sources 233 (2013) 209–215.

[39] N.Q. Hai, H. Kim, I.S. Yoo, J. Hur, Facile and scalable preparation of a MoS2/carbon nanotube nanocomposite anode for high-performance lithium-ion batteries: effects of carbon nanotube content, J. Nanosci. Nanotechnol. 19 (3) (2019) 1494–1499.

[40] Y. Choi, S. Cho, Y.-S. Lee, Effect of the addition of carbon black and carbon nanotube to FeS2 cathode on the electrochemical performance of thermal battery, J. Ind. Eng. Chem. 20 (5) (2014) 3584–3589.

[41] A. Battigelli, C. Ménard-Moyon, T. Da Ros, M. Prato, A. Bianco, Endowing carbon nanotubes with biological and biomedical properties by chemical modifications, Adv. Drug Deliv. Rev. 65 (15) (2013) 1899–1920.

[42] N. Zhang, J. Xie, V.K. Varadan, Functionalization of carbon nanotubes by potassium permanganate assisted with phase transfer catalyst, Smart Mater. Struct. 11 (6) (2002) 962.

[43] G. Sun, Z. Liu, G. Chen, Dispersion of pristine multi-walled carbon nanotubes in common organic solvents, Nano 5 (02) (2010) 103–109.

[44] E. Najafi, J.-Y. Kim, S.-H. Han, K. Shin, UV-ozone treatment of multi-walled carbon nanotubes for enhanced organic solvent dispersion, Colloids Surf. A Physicochem. Eng. Asp. 284 (2006) 373–378.

[45] J.L. Bahr, E.T. Mickelson, M.J. Bronikowski, R.E. Smalley, J.M. Tour, Dissolution of small diameter single-wall carbon nanotubes in organic solvents? Chem. Commun. 2 (2001) 193–194.

[46] R. Palanisamy, D. Karuppiah, S. Venkatesan, S. Mani, M. Kuppusamy, S. Marimuthu, A. Karuppanan, R. Govindaraju, S. Marimuthu, S. Rengapillai, M. Abdollahifar, A.K. Anbalagan, R. Perumalsamy, High-performance asymmetric supercapacitor fabricated with a novel MoS2/Fe2O3/graphene composite electrode, Colloid Interface Sci. Commun. 46 (2022), 100573.

[47] K.F. Kapiamba, Mini-review of the microscale phenomena during emulsification of highly concentrated emulsions, Colloid Interface Sci. Commun. 47 (2022), 100597.

[48] M.S. Islam, S. Mitra, Development of nano structured graphene oxide incorporated dexamethasone with enhanced dissolution, Colloid Interface Sci. Commun. 47 (2022), 100599.

[49] M. Singh, S. Rana, A.K. Singh, Advanced nanomaterials utilized as top transparent electrodes in semi-transparent photovoltaic, Colloid Interface Sci. Commun. 46 (2022), 100563.

[50] A. Abbasi Moud, Recent advances in utility of artificial intelligence towards multiscale colloidal based materials design, Colloid Interface Sci. Commun. 47 (2022), 100595.

[51] G.-X. Chen, Y. Li, H. Shimizu, Ultrahigh-shear processing for the preparation of polymer/carbon nanotube composites, Carbon 45 (12) (2007) 2334–2340.

[52] R. Andrews, D. Jacques, M. Minot, T. Rantell, Fabrication of carbon multiwall nanotube/polymer composites by shear mixing, Macromol. Mater. Eng. 287 (6) (2002) 395–403.

[53] E.T. Thostenson, T.-W. Chou, Aligned multi-walled carbon nanotube-reinforced composites: processing and mechanical characterization, J. Phys. D. Appl. Phys. 35 (16) (2002) L77.

[54] Z. Luo, J. Koo, Quantitative study of the dispersion degree in carbon nanofiber/polymer and carbon nanotube/polymer nanocomposites, Mater. Lett. 62 (20) (2008) 3493–3496.

[55] M.L. Gupta, S.A. Sydlik, J.M. Schnorr, D.J. Woo, S. Osswald, T.M. Swager, D. Raghavan, The effect of mixing methods on the dispersion of carbon nanotubes during the solvent-free processing of multiwalled carbon nanotube/epoxy composites, J. Polym. Sci. B Polym. Phys. 51 (6) (2013) 410–420.

[56] X. Yan, H. Dong, Z. Xiao, Y. Liu, T. Liu, H.G. Chae, S. Kumar, Effect of high-shear mixing by twin-screw extruder on the dispersion and homogeneity of polyacrylonitrile/carbon nanotube composite solution, Polym. Compos. 38 (4) (2017) 719–726.

[57] F. Inam, T. Vo, J.P. Jones, X. Lee, Effect of carbon nanotube lengths on the mechanical properties of epoxy resin: an experimental study, J. Compos. Mater. 47 (19) (2013) 2321–2330.

[58] Q. Cheng, S. Debnath, E. Gregan, H.J. Byrne, Ultrasound-assisted SWNTs dispersion: effects of sonication parameters and solvent properties, J. Phys. Chem. C 114 (19) (2010) 8821–8827.

[59] A. Montazeri, M. Chitsazzadeh, Effect of sonication parameters on the mechanical properties of multi-walled carbon nanotube/epoxy composites, Mater. Des. (1980–2015) 56 (2014) 500–508.

[60] K. Yang, Z. Yi, Q. Jing, R. Yue, W. Jiang, D. Lin, Sonication-assisted dispersion of carbon nanotubes in aqueous solutions of the anionic surfactant SDBS: the role of sonication energy, Chin. Sci. Bull. 58 (17) (2013) 2082–2090.

[61] A. Montazeri, N. Montazeri, K. Pourshamsian, A. Tcharkhtchi, The effect of sonication time and dispersing medium on the mechanical properties of multiwalled carbon nanotube (MWCNT)/epoxy composite, Int. J. Polym. Anal. Charact. 16 (7) (2011) 465–476.

[62] S. Gao, B.S. Villacorta, L. Ge, T.E. Rufford, Z. Zhu, Effect of sonication and hydrogen peroxide oxidation of carbon nanotube modifiers on the microstructure of pitch-derived activated carbon foam discs, Carbon 124 (2017) 142–151.

[63] J. Zou, L. Liu, H. Chen, S.I. Khondaker, R.D. McCullough, Q. Huo, L. Zhai, Dispersion of pristine carbon nanotubes using conjugated block copolymers, Adv. Mater. 20 (11) (2008) 2055–2060.

[64] J. Lee, M. Kim, C.K. Hong, S.E. Shim, Measurement of the dispersion stability of pristine and surface-modified multiwalled carbon nanotubes in various nonpolar and polar solvents, Meas. Sci. Technol. 18 (12) (2007) 3707.

[65] H.-S. Kim, M. Kang, W.-I. Park, D.-Y. Kim, H.-J. Jin, Dispersity and stability measurement of functionalized multiwalled carbon nanotubes in alcohols, Mod. Phys. Lett. B 22 (25) (2008) 2493–2501.

[66] F.V. Ferreira, W. Francisco, B.R.C. de Menezes, L.D.S. Cividanes, A. dos Reis Coutinho, G.P. Thim, Carbon nanotube functionalized with dodecylamine for the effective dispersion in solvents, Appl. Surf. Sci. 357 (2015) 2154–2159.

[67] M. Pundir, P. Prasher, K. Vasić, M. Leitgeb, A. Kumar, R. Prakash, Ž. Knez, J. K. Pandey, S. Kumar, Enzyme modified CNTs for biosensing application: opportunities and challenges, Colloid Interface Sci. Commun. 44 (2021), 100506.

[68] S. Capula-Colindres, G. Terán, E. Torres-Santillán, K. Aguir, O.G. Súchil, J. C. Velázquez, J. Oliva, Vapor-phase impregnation decomposition technique as an alternativeto decorate MWCNTs withPt and PdNPs for ammonia gas detection, Colloid Interface Sci. Commun. 44 (2021), 100490.

[69] Q. Li, M. Zaiser, V. Koutsos, Carbon nanotube/epoxy resin composites using a block copolymer as a dispersing agent, Phys. Status Solid A 201 (13) (2004) R89–R91.

[70] H. Xia, M. Song, Preparation and characterization of polyurethane–carbon nanotube composites, Soft Matter 1 (5) (2005) 386–394.

[71] V. Rezazadeh, M.R. Pourhossaini, A. Salimi, Effect of amine-functionalized dispersant on cure and electrical properties of carbon nanotube/epoxy nanocomposites, Prog. Org. Coat. 111 (2017) 389–394.

[72] W. Yuan, J. Che, M.B. Chan-Park, A novel polyimide dispersing matrix for highly electrically conductive solution-cast carbon nanotube-based composite, Chem. Mater. 23 (18) (2011) 4149–4157.

[73] M. Yin, L. Shi, D. Zhang, A. Liang, X. Sun, New insights into the “unzippering” mechanism of carbon nanotube dispersion via the “trigger” effect of small charged molecules, Colloid Interface Sci. Commun. 43 (2021), 100456.

[74] A.K.M.M. Alam, M.D.H. Beg, R.M. Yunus, M.R. Islam, Q.T.H. Shubhra, Tailoring the dispersibility of non-covalent functionalized multi-walled carbon nanotube (MWCNT) nanosuspension using shellac (SL) bio-resin: structure-property relationship and cytotoxicity of shellac coated carbon nanotubes (SLCNTs), Colloid Interface Sci. Commun. 42 (2021), 100395.

[75] N. Rahmati, M. Rahimnejad, M. Pourali, S.K. Muallah, Effective removal of nickel ions from aqueous solution using multi-wall carbon nanotube functionalized by glycerol-based deep eutectic solvent, Colloid Interface Sci. Commun. 40 (2021), 100347.
[76] M. Davardoostmanesh, H. Ahmadzadeh, E.K. Goharshadi, Preparation of monodispersed carbonaceous nanomaterials – a review, Colloid Interface Sci. Commun. 44 (2021), 100479.
[77] P. Yadav, S.M. Gupta, S. Sharma, A review on stabilization of carbon nanotube nanofluid, J. Therm. Anal. Calorim. (2021) 1–25.
[78] Y. Kim, J.S. Hong, S.Y. Moon, J.-Y. Hong, J.U. Lee, Evaluation of carbon nanotubes dispersion in aqueous solution with various dispersing agents, Carbon Lett. 31 (6) (2021) 1327–1337.
[79] Y. Geng, M.Y. Liu, J. Li, X.M. Shi, J.K. Kim, Effects of surfactant treatment on mechanical and electrical properties of CNT/epoxy nanocomposites, Compos. A: Appl. Sci. Manuf. 39 (12) (2008) 1876–1883.
[80] A. Amiri, M. Shanbedi, H. Eshghi, S.Z. Heris, M. Baniadam, Highly dispersed multiwalled carbon nanotubes decorated with Ag nanoparticles in water and experimental investigation of the thermophysical properties, J. Phys. Chem. C 116 (5) (2012) 3369–3375.
[81] Z. Huang, L. Xi, Q. Subhani, W. Yan, W. Guo, Y. Zhu, Covalent functionalization of multi-walled carbon nanotubes with quaternary ammonium groups and its application in ion chromatography, Carbon 62 (2013) 127–134.
[82] L. Bai, Z. Li, S. Zhao, J. Zheng, Covalent functionalization of carbon nanotubes with hydroxyl-terminated polydimethylsiloxane to enhance filler dispersion, interfacial adhesion and performance of poly (methylphenylsiloxane) composites, Compos. Sci. Technol. 165 (2018) 274–281.
[83] B. Vigolo, V. Mamane, F. Valsaque, T.H. Le, J. Thabit, J. Ghanbaja, L. Aranda, Y. Fort, E. McRae, Evidence of sidewall covalent functionalization of single-walled carbon nanotubes and its advantages for composite processing, Carbon 47 (2) (2009) 411–419.
[84] S. Hong, M. Kim, C.K. Hong, D. Jung, S.E. Shim, Encapsulation of multi-walled carbon nanotubes by poly (4-vinylpyridine) and its dispersion stability in various solvent media, Synth. Met. 158 (21–24) (2008) 900–907.
[85] M. Raimondo, C. Naddeo, L. Vertuccio, L. Bonnaud, P. Dubois, W.H. Binder, A. Sorrentino, L. Guadagno, Multifunctionality of structural nanohybrids: the crucial role of carbon nanotube covalent and non-covalent functionalization in enabling high thermal, mechanical and self-healing performance, Nanotechnology 31 (22) (2020), 225708.
[86] P. Bilalis, D. Katsigiannopoulos, A. Avgeropoulos, G. Sakellariou, Non-covalent functionalization of carbon nanotubes with polymers, RSC Adv. 4 (6) (2014) 2911–2934.
[87] C. Damian, S. Garea, E. Vasile, H. Iovu, Covalent and non-covalent functionalized MWCNTs for improved thermo-mechanical properties of epoxy composites, Compos. Part B 43 (8) (2012) 3507–3515.
[88] C.Y. Hu, Y.J. Xu, S.W. Duo, R.F. Zhang, M.S. Li, Non-covalent functionalization of carbon nanotubes with surfactants and polymers, J. Chin. Chem. Soc. 56 (2) (2009) 234–239.
[89] A.A. Hofstra, M.L. Morris, J.L. Sample, W.D. Powell, Non-covalent functionalized nanotubes in nylon 12, in: Physical Chemistry of Interfaces and Nanomaterials VI, SPIE, 2007, pp. 7–15.
[90] M.A. Saleemi, M.H. Fouladi, P.V.C. Yong, E.H. Wong, Elucidation of antimicrobial activity of non-covalently dispersed carbon nanotubes, Materials 13 (7) (2020) 1676.
[91] D. Tuncel, Non-covalent interactions between carbon nanotubes and conjugated polymers, Nanoscale 3 (9) (2011) 3545–3554.
[92] D. Ratna, T. Abraham, S. Siengchin, J. Karger-Kocsis, Novel method for dispersion of multiwall carbon nanotubes in poly (ethylene oxide) matrix using dicarboxylic acid salts, J. Polym. Sci. B Polym. Phys. 47 (12) (2009) 1156–1165.
[93] X. Chen, X. Yu, Y. Liu, J. Zhang, Stepwise design of non-covalent wrapping of large diameter carbon nanotubes by peptides, J. Mol. Graph. Model. 46 (2013) 83–92.
[94] E. Cohen, H. Dodiuk, A. Ophir, S. Kenig, C. Barry, J. Mead, Evidences for π-interactions between pyridine modified copolymer and carbon nanotubes and its role as a compatibilizer in poly (methyl methacrylate) composites, Compos. Sci. Technol. 79 (2013) 133–139.
[95] H. Lee, M.N. Kim, H.G. Jang, J.-U. Jang, J. Kim, S.Y. Kim, Phenyl glycidyl ether-based non-covalent functionalization of nano-carbon fillers for improving conductive properties of polymer composites, Compos. Commun. 33 (2022), 101237.
[96] Y. Ren, Z. Zhou, G. Yin, G.-X. Chen, Q. Li, Effect of ionic liquid-containing poly (ε-caprolactone) on the dispersion and dielectric properties of polymer/carbon nanotube composites, RSC Adv. 6 (37) (2016) 31351–31358.
[97] A. Zhang, J. Luan, Y. Zheng, L. Sun, M. Tang, Effect of percolation on the electrical conductivity of amino molecules non-covalently coated multi-walled carbon nanotubes/epoxy composites, Appl. Surf. Sci. 258 (22) (2012) 8492–8497.
[98] J. Zhao, J. Ma, X. Nan, B. Tang, Application of non-covalent functionalized carbon nanotubes for the counter electrode of dye-sensitized solar cells, Org. Electron. 30 (2016) 52–59.
[99] N. Mohd Nurazzi, M.M. Asyraf, A. Khalina, N. Abdullah, F.A. Sabaruddin, S. H. Kamarudin, S.B. Ahmad, A.M. Mahat, C.L. Lee, H. Aisyah, Fabrication, functionalization, and application of carbon nanotube-reinforced polymer composite: an overview, Polymers 13 (7) (2021) 1047.
[100] J.A. Fagan, B.J. Bauer, E.K. Hobbie, M.L. Becker, A.R. Hight Walker, J. R. Simpson, J. Chun, J. Obrzut, V. Bajpai, F.R. Phelan, Carbon nanotubes: measuring dispersion and length, Adv. Mater. 23 (3) (2011) 338–348.
[101] D. Zhang, Y. Huang, Dispersion characterizations and adhesion properties of epoxy composites reinforced by carboxymethyl cellulose surface treated carbon nanotubes, Powder Technol. 117505 (2022).
[102] A.H. Korayem, M.R. Barati, S.J. Chen, G.P. Simon, X.L. Zhao, W.H. Duan, Optimizing the degree of carbon nanotube dispersion in a solvent for producing reinforced epoxy matrices, Powder Technol. 284 (2015) 541–550.
[103] A. Zalewska, J. Kowalik, I. Grubecki, Application of turbiscan lab to study the effect of emulsifier content on the stability of plant origin dispersion, Chem. Process. Eng. 40 (4) (2019) 399–409.
[104] X.-F. Guo, G.-J. Kim, Synthesis of ultrafine carbon black by pyrolysis of polymers using a direct current thermal plasma process, Plasma Chem. Plasma Process. 30 (1) (2010) 75–90.
[105] A. Abubakar Umar, I. Mohd Saaid, A. Adebayo Sulaimon, R. Mohd Pilus, N. A. Amer, A. Halilu, B. Mamo Negash, Characterization of Native Colloids and Study of Emulsions Stabilized by Asphaltene, Wax, Silicates and Calcites Using Optical Analyzer Turbiscan, SPE Middle East Oil and Gas Show and Conference, OnePetro, 2019.
[106] Y.-T. Kwon, Y.-M. Choi, K.-H. Kim, C.-G. Lee, K.-J. Lee, B.-S. Kim, Y.-H. Choa, Synthesis of CdSe/ZnSe quantum dots passivated with a polymer for oxidation prevention, Surf. Coat. Technol. 259 (2014) 83–86.
[107] H.-S. Kim, W.-I. Park, M. Kang, H.-J. Jin, Multiple light scattering measurement and stability analysis of aqueous carbon nanotube dispersions, J. Phys. Chem. Solids 69 (5–6) (2008) 1209–1212.
[108] K. Seffaha, Setting in Suspension of Double-Walled Carbon by Some Biopolymers: Characterization by Turbiscan, 2022.
[109] J. Kwon, J. Kim, S.Y. Bae, S.P. Jeon, J.H. Song, S.E. Wang, D.S. Jung, J. Jang, H. Park, P.J. Kim, Polyanion-assisted ionic-electronic conductive agents designed for high density Si-based anodes, J. Power Sources 541 (2022), 231728.
[110] G. Wang, J. Yang, Y. Wang, Y. Liu, Self-assembly behavior of carbon nanotubes modified by amphiphilic block copolymer, Colloid Polym. Sci. 288 (18) (2010) 1677–1685.
[111] B.-S. Kim, D. Kim, K.-W. Kim, T. Lee, S. Kim, K. Shin, S. Chun, J.H. Han, Y.S. Lee, H.-J. Paik, Dispersion of non-covalently functionalized single-walled carbon nanotubes with high aspect ratios using poly (2-dimethylaminoethyl methacrylate-co-styrene), Carbon 72 (2014) 57–65.
[112] T. Lee, B. Kim, S. Kim, J.H. Han, H.B. Jeon, Y.S. Lee, H.-J. Paik, Fabrication of flexible, transparent and conductive films from single-walled carbon nanotubes with high aspect ratio using poly ((furfuryl methacrylate)-co-(2-(dimethylamino) ethyl methacrylate)) as a new polymeric dispersant, Nanoscale 7 (15) (2015) 6745–6753.
[113] H. Ha, R. Thompson, P. Matteini, S.J. Yoo, B. Hwang, Effect of surface change by vacuum drying on the sedimentation stability of iron nanoparticles in volatile organic solvents, Colloid Interface Sci. Commun. 48 (2022), 100625.
[114] G. Zhang, Y. Chen, X. Sui, M. Kang, Y. Feng, H. Yin, Nonionic surfactant stabilized polytetrafluoroethylene dispersion: effect of molecular structure and topology, J. Mol. Liq. 345 (2022), 116988.
[115] M. Mazloumi, L.J. Johnston, Z.J. Jakubek, Dispersion, stability and size measurements for cellulose nanocrystals by static multiple light scattering, Cellulose 25 (10) (2018) 5751–5768.
[116] H. Ha, R. Thompson, B. Hwang, Iron oxide layer effects on the sedimentation behavior of carbonyl iron powder suspension, Colloid and Interface Science Communications 50 (2022) 100670.
[117] Z.Q. Liu, X. Yang, Q. Zhang, TURBISCAN: history, development, application to colloids and dispersions, Adv. Mater. Res. Trans. Tech. Publ. (2014) 1592–1596.
[118] Y. Sun, A. Deac, G.G. Zhang, Assessing physical stability of colloidal dispersions using a turbiscan optical analyzer, Mol. Pharm. 16 (2) (2019) 877–885.
[119] J. Hong, C. Kook Hong, S. Choe, S. Eun Shim, Preparation of poly (acrylamide)/MWNTs nanocomposite using carboxylated MWNTs, J. Polym. Sci. A Polym. Chem. 45 (15) (2007) 3477–3481.
[120] D. Seo, W. Yoon, S. Park, M. Jo, J. Kim, The preparation of multi-walled CNT-PMMA nanocomposite, Carbon lett. 7 (4) (2006) 266–270.
[121] A. Haywood, The Effect of Polymer Solutions on the Settling Behaviour of Sand Particles, The University of Manchester, 2011.
[122] T.F. Tadros, Basic Principles of Formulation Types, Walter de Gruyter GmbH & Co KG, 2018.
[123] D.-Y. Kim, R. Jung, H.-S. Kim, H.-J. Jin, Electrically conductive polymeric nanocomposites prepared in alcohol dispersion of multiwalled carbon nanotubes, Mol. Cryst. Liq. Cryst. 491 (1) (2008) 255–263.
[124] Y. Kim, S.-M. Kwon, D.-Y. Kim, H.-S. Kim, H.-J. Jin, Dispersity and stability measurements of functionalized multiwalled carbon nanotubes in organic solvents, Curr. Appl. Phys. 9 (2) (2009) e100–e103.
[125] S.W. Lee, B.-S. Kim, S. Chen, Y. Shao-Horn, P.T. Hammond, Layer-by-layer assembly of all carbon nanotube ultrathin films for electrochemical applications, J. Am. Chem. Soc. 131 (2) (2009) 671–679.
[126] G. Wang, Y. Liu, Self-assembly of carbon nanotubes modified by amphiphilic block polymers in selective solvent, Macromol. Chem. Phys. 210 (23) (2009) 2070–2077.
[127] M. Han, Z.-H. Zhou, Y.-L. Luo, F. Xu, Y.-S. Chen, pH-sensitive carbon nanotubes graft polymethylacrylic acid self-assembly nanoplatforms for cellular drug release, J. Biomater. Appl. 37 (4) (2022) 737–750.
[128] J. Zhu, M. Yudasaka, M. Zhang, S. Iijima, Dispersing carbon nanotubes in water: a noncovalent and nonorganic way, J. Phys. Chem. B 108 (31) (2004) 11317–11320.
[129] Y. Seo, H. Ha, J.Y. Cheong, M. Leem, S. Darabi, P. Matteini, C. Müller, T.G. Yun, B. Hwang, Highly reliable yarn-type supercapacitor using conductive silk yarns with multilayered active materials, J. Nat. Fibers 19 (3) (2022) 835–846.

[130] T. Fujigaya, N. Nakashima, Non-covalent polymer wrapping of carbon nanotubes and the role of wrapped polymers as functional dispersants, Sci. Technol. Adv. Mater. 16 (2) (2015), 024802.
[131] D. Ponnamma, S.H. Sung, J.S. Hong, K.H. Ahn, K. Varughese, S. Thomas, Influence of non-covalent functionalization of carbon nanotubes on the rheological behavior of natural rubber latex nanocomposites, Eur. Polym. J. 53 (2014) 147–159.
[132] L. Jiang, L. Gao, J. Sun, Production of aqueous colloidal dispersions of carbon nanotubes, J. Colloid Interface Sci. 260 (1) (2003) 89–94.
[133] T. Lee, J. Park, K. Kim, A.K. Mohanty, B. Kim, J.H. Han, H.B. Jeon, Y.S. Lee, H.-J. Paik, Facile tuning of a polymeric dispersant for single-walled carbon nanotube dispersion, RSC Adv. 5 (85) (2015) 69410–69417.